Proceedings 10th NUMGE 2023
10th European Conference on Numerical Methods in Geotechnical Engineering
Zdravkovic L, Kontoe S, Taborda DMG, Tsiampousi A (eds)

https://doi.org/10.53243/NUMGE2023-151

Evaluation of a Gauss integration scheme in MPM for strain-dependent soils

M. Martinelli[1,2], G. Remmerswaal[2]

[1] *Faculty of Civil Engineering and Geosciences, Delft University of Technology, Delft, the Netherlands*
[2]*Geo-Engineering Unit, Deltares, Delft, The Netherlands*

ABSTRACT: A realistic quantification of the probability of flooding for dike assessment requires the calculation of the complete failure process after slope instability, which can be modelled using for example the Material Point Method (MPM). For the assessment of realistic cases, complex geometries must be modelled, and strain-softening behaviour must be taken into account. The MPM formulation proposed by Martinelli and Galavi (2022) is capable of modelling complex geometries, but it has limitations when strain-softening constitutive models are adopted. In this formulation, the state variables are averaged within each computational element, and softening is distributed among material points as result of the element averaging. Therefore, softening can occur in material points which did not experience high deviatoric strains. In this paper, a new MPM integration scheme is proposed, developed within the same framework, but it does not modify state variables in the material points due to element averaging. An example of soil column collapse is illustrated in this paper, which develops multiple failure mechanisms (progressive failure), and it highlights that the new formulation indeed prevents distribution of softening behaviour. This MPM approach can, in a following study, be used to assess the failure process of a real dike.

Keywords: Dike slope stability; Material Point Method; Strain-softening; Gauss integration; MPM-GP

1 INTRODUCTION

In the former Dutch dike safety assessments (before 2017), it is conservatively assumed that a single dike slope instability always leads to flooding. The assessments did not consider the resistance against flooding which may be present after initial failure. In essence, it is not considered that severe damage to the dike body (e.g., by retrogressive slope failure) is necessary before a breach occurs. After 2017, the Dutch safety assessments consider the probability of flooding, and allows to include the contribution of the secondary failure mechanisms. However, a full understanding of the failure processes after initial failure is lacking, and reliable tools to analyse and quantify the secondary failure mechanisms are not yet developed.

Van der Krogt et al. (2019) proposed a practical method to assess secondary failure mechanisms, by estimating the damaged profile of the dike, and assessing the probability of failure of this profile with the limit equilibrium method (LEM). However, the damaged geometry was determined based on simple assumptions or rules-of-thumb.

Remmerswaal et al (2021) used the Material Point Method (MPM), to perform a probabilistic assessment of the complete failure process, thereby improving the assessment of the damaged geometry. The MPM formulation adopted by Remmerswaal et al (2021) requires a structured and regular computational mesh, which can only be used for relatively simple geometries. A stable MPM formulation for unstructured mesh is required to make MPM applicable to most problems. Martinelli and Galavi (2022), therefore, proposed a MPM formulation for unstructured quadrilateral meshes. This formulation mitigates stress oscillations using a Gauss integration scheme, and volumetric locking using a reduced integration technique. The scheme has been shown to be successful in many applications, such as a dam break, bearing capacity and CPT testing (Martinelli and Galavi (2022)).

The aim of this paper is to further extend the MPM formulation proposed by Martinelli and Galavi (2022), when considering strain-softening models. The paper illustrates the results of the simulations of a large soil column failure, highlighting limitations of this MPM scheme in case of strain-softening materials. A new formulation is proposed, developed within the same framework of Martinelli and Galavi (2022), preventing some of the limitations of the existing framework for strain-softening soil response.

2 MPM FORMULATIONS

2.1 MPM-Mixed

Martinelli and Galavi (2022) adopted an integration scheme which mitigates stress oscillation, here called

MPM-Mixed, where Gauss points in 4-node quadrilateral elements are used to compute the internal force. The 4-node quadrilateral element is divided into four sub-elements, one for each Gauss point (GP), defined based on the local coordinates. The stress tensor at each of the four GPs (σ_{GP}) is calculated as the weighted average of the stress tensors of all material points in the sub-element, as follows:

$$\sigma_{GP} = \frac{\sum_{MP=1}^{N_{MP,GP}} \sigma_{MP} \Omega_{\mathrm{MP}}}{\sum_{\mathrm{MP}=1}^{N_{MP,GP}} \Omega_{MP}} \quad (1)$$

where σ_{MP} and Ω_{MP} are the stress and the integration weight of the material point, respectively.

The stress tensor of the GP is then corrected with a similar technique adopted in FLAC (Itasca, 2016): the isotropic part of the stress tensor (p_{GP}) is weighted averaged over the entire element (p_{el}) and the deviatoric part is recalculated accordingly:

$$p_{el} = \frac{\sum_{GP=1}^{N_{GP}} p_{GP} \Omega_{\mathrm{GP}}}{\Omega_{el}} \quad (2)$$

$$\hat{\sigma}_{GP} = \sigma_{GP,1} - \left(\frac{1}{3} tr\left(\sigma_{GP}\right) - p_{el}\right) I \quad (3)$$

The GP stress ($\hat{\sigma}_{GP}$) is then updated as a function of the strain increment computed at the corresponding Gauss point. For nearly-incompressible materials, the B-bar method (Hughes, T.J.R., 2000) is used to mitigate volumetric locking: the deviatoric strain increments are calculated in all four Gauss points, but only one Gauss point, located in the center of the element, is used for the volumetric strains.

Lastly, the stress tensor of the gauss point ($\hat{\sigma}_{GP}$) is then assigned back to all material points in the sub-element.

State variables

When an advanced constitutive model is used, the state variables (α_{GP}) are also mapped to the Gauss point (Eq. (1)) and assigned back to the MPs in each sub-element. The isotropic state variables are averaged over the entire element (Eq. (2)). The main limitation of this approach, as mentioned in the original paper of Martinelli and Galavi (2022), is that the history of the material points is lost as the state variables are replaced every timestep.

Internal force

The internal force vector in *MPM-Mixed* is integrated according to the Gauss point variables as follows:

$$f_i^{int} = \sum_{el=1}^{N_{el,i}} \sum_{GP=1}^{N_{GP,el}} B_i^T(\xi_{GP}) \hat{\sigma}_{GP} \, \Omega_{GP} \quad (4)$$

where ξ_{GP} is the local coordinate of the Gauss point in the element and $N_{GP,el}$ is the number of Gauss points in the element.

Stress integration

The following procedure is used to integrate the stress of the material points from the nodal velocities:

1. Define the initial stress and state variables at the gauss point, using Eqs. (1), (2) and (3) ($\hat{\sigma}_{GP,0}, \alpha_{GP,0}$).
2. Compute strain at Gauss points from nodal velocities. B-bar method is used for incompressible materials.
3. Compute new stress and state variables at the gauss point using the constitutive model ($\hat{\sigma}_{GP,1}, \alpha_{GP,1}$).
4. Assign the updated GP stress and state variables to the MPs: $\sigma_{MP,1} = \hat{\sigma}_{GP,1}$ and $\alpha_{MP,1} = \alpha_{GP,1}$.

2.2 MPM-GP

The proposed new MPM formulation is described in this section, named *MPM-GP*. In *MPM-GP*, the gauss point initial stress and strain are computed like *MPM-Mixed* (i.e. step 1-2 in Stress Integration). As in *MPM-Mixed,* the gauss point stresses are also used to determine the internal forces (Eq. (4)). To ensure that the history of the material point is not lost due to the transfer the stresses and state variables from the gauss point to the material points (Step 4), Steps 3 and 4 are not performed. Instead, the new stress and state variables are calculated in each material point using the strain increment at each Gauss point ($\hat{\sigma}_{MP,1}, \alpha_{MP,1}$).

3 PROBLEM DESCRIPTION

The *MPM-Mixed* and *MPM-GP* formulations are used to study the failure of a large soil column. A 8 meter wide and 2 meter high soil column, see Figure 1, is unstable under its own weight. The column is discretized using 0.1 m x 0.1 m background grid elements, i.e. 20 elements are used in the vertical directions. Each element initially contains 25 equally spaced material points (5 in each direction).

The material response is simulated using a Tresca strain-softening constitutive model, with an initial peak undrained shear strength $S_{u,0}$ of 8 kPa. Two models are studied. In *model 1*, no softening is used, i.e. the residual undrained shear strength $S_{u,r}$ is also set to 8 kPa. In *model 2*, the value of $S_{u,r}$ is set to 2 kPa. The transition between the peak to residual strength is defined using an exponential relationship, which relates the strength S_u to the accumulated equivalent plastic strains $\varepsilon_{eq,p}$, defined as follows:

$$S_u = S_{u,r} + (S_{u,p} - S_{u,r}) e^{\eta \, \varepsilon_{eq,p}} \quad (5)$$

$$\varepsilon_{eq,p} = \sum \sqrt{\frac{1}{2} d\boldsymbol{e_p} \cdot d\boldsymbol{e_p}} \quad (6)$$

where $d\boldsymbol{e_p}$ is the deviatoric part of the increment of the plastic strain tensor, and η is the shape factor, set to 50. The $S_{u,95}$ (which corresponds to 95% reduction of the shear strength) is reached after approximately 6% of accumulated plastic shear strain.

The material has a porosity of 0.4, a density of 1990 kg/m^3, a shear modulus of 2000 kPa and a Poisson's ratio of 0.48. Volumetric locking is mitigated using the B-bar method. A viscous damping, with a damping factor set to 0.1, is adopted in all simulations.

A roller boundary is placed at the left (and right) edge of the domain. A contact boundary is used along the bottom boundary. In *model 1*, this boundary is perfectly smooth, i.e. it acts as roller boundary, whereas in *model 2*, the adhesion is set to 8 kPa. A roller boundary has been used in *model 1* to cause large deformations.

The failure process is described hereafter. For only *model 2*, 10 material points are selected to analyze in detail the evolution of the total deviatoric strain and cumulative plastic deviatoric strain (i.e. the state variable of the constitutive model) during the analysis. The initial position of these target material points is illustrated in Figure 1 and summarized in Table 1.

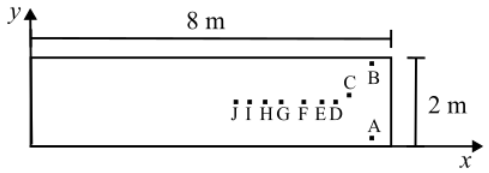

Figure 1. Problem geometry including the initial position of the output material points.

Table 1: Initial position of the output material points

Material point	x-coordinate	y-coordinate
A	7.60 m	0.07 m
B	7.60 m	1.93 m
C	7.13 m	1.09 m
D	6.90 m	1.00 m
E	6.60 m	1.00 m
F	6.00 m	1.00 m
G	5.50 m	1.00 m
H	5.20 m	1.00 m
I	4.70 m	1.00 m
J	4.50 m	1.00 m

4 RESULTS

4.1 Model 1 – No softening

Figure 2 and Figure 3 show the deformed configuration at several time instants (t=1 and 2 s) during the failure process, and at the end of failure (t=4s). The distribution of the total deviatoric strains is in Figure 2, and the distribution of $\varepsilon_{eq,p}$ is in Figure 3. The results show that both *MPM-Mixed* and *MPM-GP* formulations provide very similar failure pattern and strain distribution for the column collapse in case of no-softening material response.

Figure 2 shows that the total deviatoric strain is smooth in both *MPM-Mixed* and *MPM-GP*, as the strains at the material points are not replaced with the values at the Gauss point. Figure 3 highlight differences in the distribution of the state variable. *MPM-Mixed* results in a piecewise constant distribution of $\varepsilon_{eq,p}$ (Figure 3a), as $\varepsilon_{eq,p}$ are averaged in the element and re-assigned to the MPs. On the contrary, *MPM-GP* provides a continuous evolution of the state variables (see Figure 3b), since GP state variables are not re-assigned to the MPs.

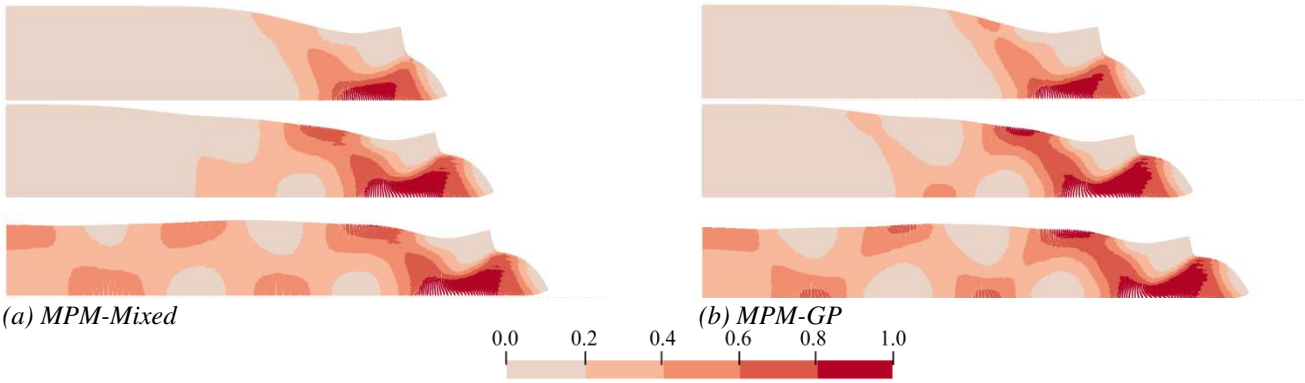

(a) MPM-Mixed *(b) MPM-GP*

Figure 2. Total deviatoric strain computed with (a) MPM-Mixed and (b) MPM-GP after 1 second, 2 seconds and 4 seconds

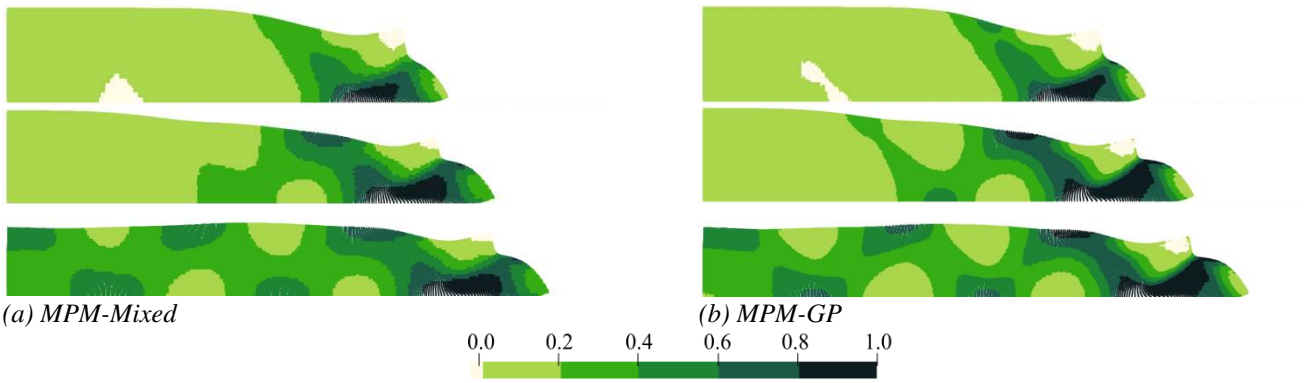

Figure 3. Accumulated equivalent plastic deviatoric strains $\varepsilon_{eq,p}$ computed with (a) MPM-Mixed and (b) MPM-GP after 1 second, 2 seconds and 4 seconds

4.2 Model 2 – With Softening

When softening is included, similar slip circles are observed in *MPM-Mixed* and *MPM-GP*, but the behaviour during failure differs significantly between *MPM-Mixed* and *MPM-GP* (see Figure 4 and Figure 5). In *MPM-Mixed* regions outside the slip surface soften during translation, while in *MPM-GP* these regions retain their strength. Since the state variable is averaged within each element in *MPM-Mixed*, material softening is spread over parts of soil that experienced different degrees of softening, as the MPs move to an element with different strain-history. Such spreading is more frequent when the soil significantly translates, crossing several background grid elements, for example in the sliding mass. Due to the averaging of state variables, wider shear bands occur in *MPM-Mixed* and a lower peak cumulative plastic deviatoric strain is observed in *MPM-Mixed* compared to *MPM-GP*.

Figure 6a and Figure 7a show a mismatch between the total and the cumulative plastic deviatoric strain in *MPM-Mixed*. The figures show that the cumulative plastic deviatoric strain can decrease when it is replaced by the average value in the element. This does not occur in *MPM-GP* (Figure 6b and Figure 7b), where $\varepsilon_{eq,p}$ can only increase (in agreement with Eq. (6)).

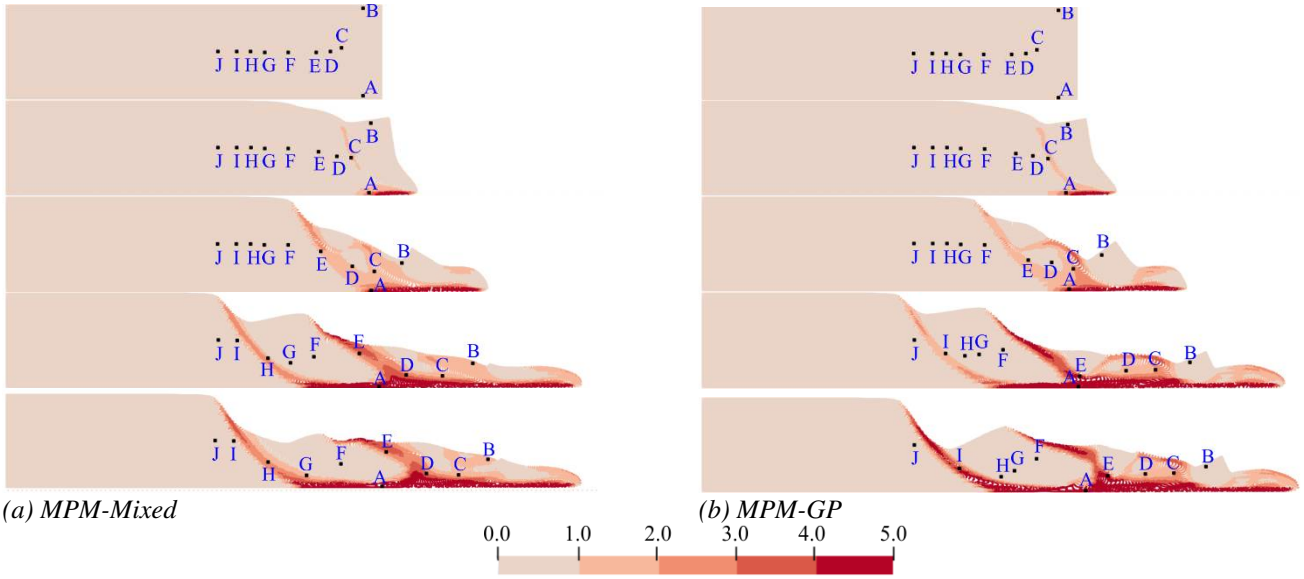

Figure 4. Total deviatoric strain at the start of the simulation (0 seconds), first failure (0.5 seconds), first failure (1.0 seconds), second failure (2.5 seconds) and at the end of the simulation (4.0 seconds). Black dots indicate the material point positions A-J

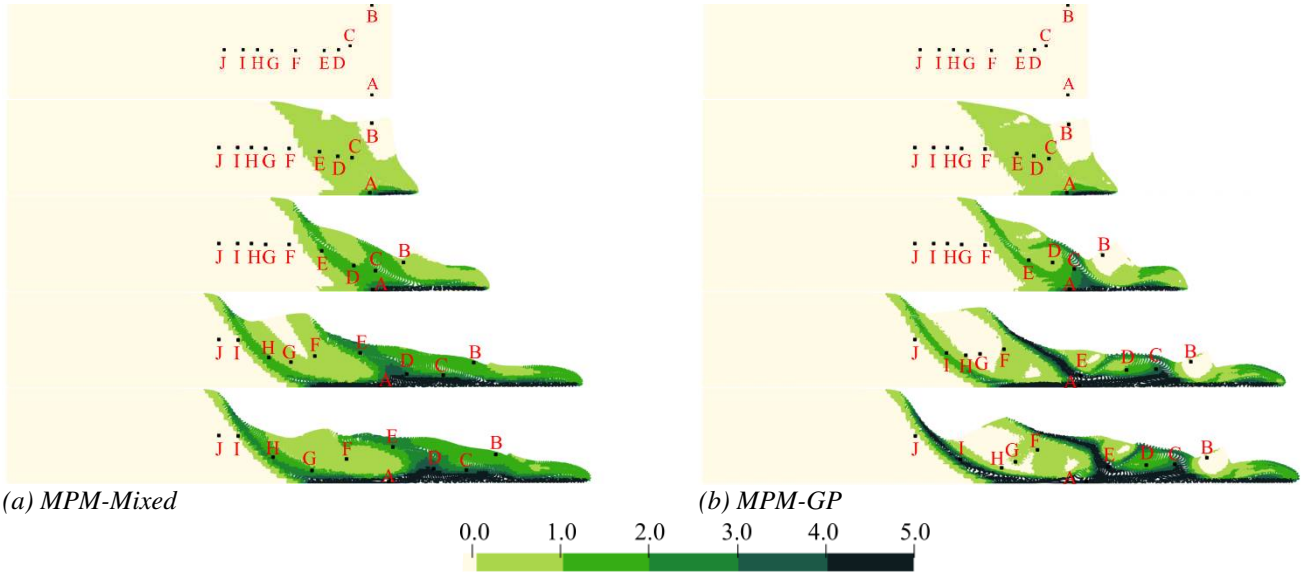

(a) MPM-Mixed *(b) MPM-GP*

Figure 5. Cumulative plastic deviatoric strain at the start of the simulation (0 seconds), first failure (0.5 seconds), first failure (1.0 seconds), second failure (2.5 seconds) and at the end of the simulation (4.0 seconds).

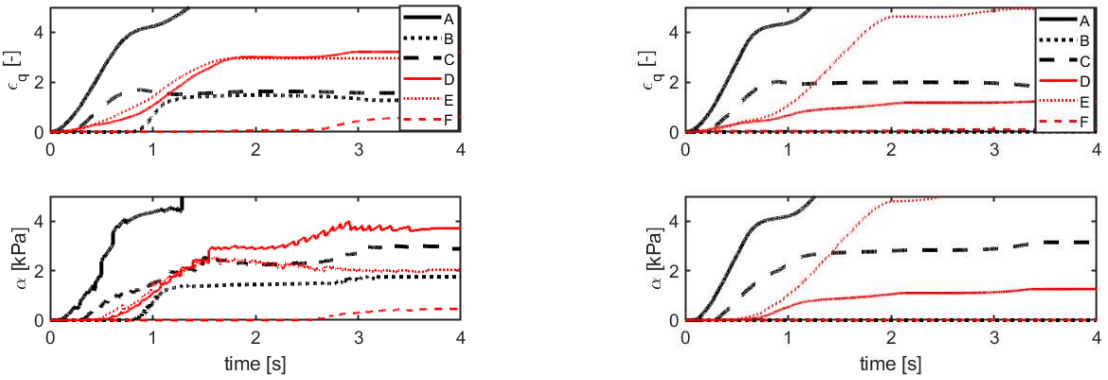

(a) *(b)*

Figure 6. Total and cumulative plastic deviatoric strain at points A-F for (a) MPM-Mixed and (b) MPM-GP.

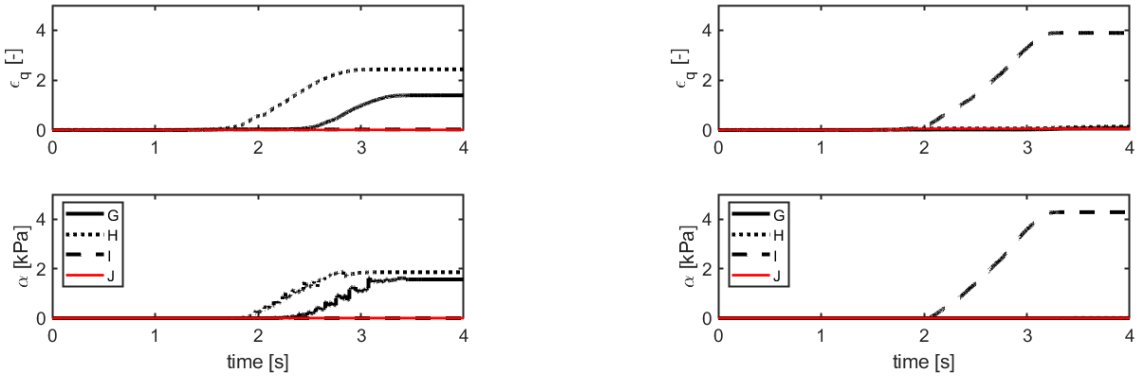

(a) *(b)*

Figure 7: Total and cumulative plastic deviatoric strain at points G-J for (a) MPM-Mixed and (b) MPM-GP.

Figure 8 and Figure 9 show the evolution of the shear strength in time. In *MPM-Mixed*, as result of element averaging, material points can gain strength in time. This cannot occur in MPM-GP, where strength can only decrease in agreement with Eq. (5)). Moreover, the strength of the material points (B and F), which are outside the first shear band, decreases lower (and at later time) in *MPM-GP* compared to *MPM-Mixed*. This confirms that softening is more likely to remain within the shear band in *MPM-GP*

The second failure occurs earlier in *MPM-Mixed* compared to *MPM-GP*, see Figure 9. The failure passes through different material points: point H in MPM-Mixed and point I in MPM-GP. This indicates that the

(a) (b)

Figure 8. Current value of the shear strength computed at points A-F for (a) MPM-Mixed and (b) MPM-GP.

(a) (b)

Figure 9. Cumulative plastic deviatoric strain and undrained shear strength computed at points G-J for (a) MPM-Mixed and (b) MPM-GP.

failure volume predicted by *MPM-Mixed* is smaller, and more soil column remains standing.

5 CONCLUSIONS

This paper presents a new MPM integration scheme (called here *MPM-GP*). It is developed within the same framework of Martinelli and Galavi (2022) (called here *MPM-Mixed*), i.e.: (1) it mitigates volumetric locking in incompressible materials by adopting the B-bar method, (2) it mitigates stress oscillations using the Gauss integration method, and (3) the method can be used with both structured and unstructured computational meshes.

The *MPM-GP* is an enhancement of the *MPM-Mixed* when dealing with strain-softening materials, as the strain-history of the soil is not lost during averaging (as in *MPM-Mixed*), but it is correctly preserved.

The performance of the integration scheme is highlighted illustrating the results of a large soil column failure. The simulations are performed considering a cohesive material, with and without strain-softening. In absence of softening, similar behaviour is observed between the two formulations. In case of strain-softening similar failure surfaces are observed, but major differences can occur during failure, since softening in *MPM-GP* is no longer spread through the domain but calculated at every material point.

In future, the *MPM-GP* formulation will be used to study a realistic dike failure, aiming at the quantification of the probability of flooding after extreme deformations and multiple failure mechanisms. Additionally, the differences between *MPM-GP* and *MPM-Mixed* will be further investigated for various problems, to highlight whether *MPM-GP* adequetly captures complex constitutive behaviour in an unstructured mesh.

It is worth mentioning that, since strain-softening material response is adopted, strain-localization occurs in the simulations and the results may be dependent on the mesh-size and mesh-orientation. For this reason, a more advanced regularization technique needs to be adopted in the numerical method to improve the quality of the results. However, the current framework can still be used as a solid basis to study the vulnerability of dikes and their capabilities to resist against flooding.

6 ACKNOWLEDGEMENTS

The authors would like to acknowledge Rijkswaterstaat-WVL for initiating and financing this research through the Kennis voor Keringen-research project.

7 REFERENCES

Hughes, T.J.R., 2000. The Finite Element Method: Linear Static and Dynamic Finite Element Analysis. Prentice-Hall, Englewood Cliffs, NJ.

van der Krogt, M.G., Schweckendiek, T., Kok, M., 2019. Do all dike instabilities cause flooding? *13th International Conference on Applications of Statistics and Probability in Civil Engineering*, *ICASP 2019*.

Martinelli, M., Galavi, V. 2022. An explicit coupled MPM formulation to simulate penetration problems in soils using quadrilateral elements. *Computers and Geotechnics* **145**.

Remmerswaal, G., Vardon, P.J., Hicks, M.A. 2021. Evaluating residual dyke resistance using the Random Material Point Method. *Computers and Geotechnics* **133**.